Targeting Semaphorin 7a signaling in preclinical models of estrogen receptor-positive breast cancer

Rachel N Steinmetz[1,2], Veronica Wessells[1], Heather Fairchild[1], Traci R Lyons[1,2,3]

[1]Division of Medical Oncology, Department of Medicine, School of Medicine, University of Colorado Anschutz Medical Campus, Aurora, CO, USA.
[2]Young Women's Breast Cancer Translational Program, University of Colorado Anschutz Medical Campus, Aurora, CO 80045, USA.
[3]University of Colorado Cancer Center, Aurora, CO, 80045, USA.

Running title: Targeting SEMA7A signaling in preclinical models of ER+ breast cancer

Corresponding author:
Name: Traci R. Lyons
Address: U. Colorado Anschutz, 12801 E 17th Ave, L18-8103 MS 8117, Aurora, CO 80045
Email: traci.lyons@cuanschutz.edu

Conflict of interest disclosures:
Rachel N Steinmetz – no conflict of interest to disclose.
Veronica Wessells – no conflict of interest to disclose.
Heather Fairchild – no conflict of interest to disclose.
Traci R Lyons – Cofounder and Chief Scientific Officer of Pearl Scientific.

TRANSLATIONAL RELEVANCE

Our studies propose inhibition of a novel target in estrogen receptor-positive (ER+) breast cancer (BC) with an anti-Semaphorin 7a (SEMA7A) monoclonal antibody (SmAbH1). We show efficacy of SmAbH1 as a single agent and in combination with endocrine therapy in preclinical models. We also show that targeting of SEMA7A signaling, including the use of well-known and novel PI3K inhibitors, could be an effective treatment strategy for patients with SEMA7A+ BC, particularly in combination with standard of care. Our mechanistic studies detail the cellular signaling pathway activated by SEMA7A and support the further investigation of these novel drug combinations for clinical use. Further, SEMA7A is a biomarker for poor prognosis and decreased patient survival, posing the need for a clinical diagnostic test for SEMA7A levels in BC patients, which we are currently developing.

ABSTRACT

Estrogen receptor-positive (ER+) breast cancer (BC) comprises over 70% of breast cancers and is the leading cause of BC-related deaths in women worldwide. Despite available therapies targeting ER in BC, recurrence occurs in many patients due to therapeutic resistance. Semaphorin 7a (SEMA7A) is a biomarker associated with poor prognosis and endocrine therapy resistance for BC patients. Survival analyses of ER+ BC patients on endocrine therapy confirm early recurrence in patients with SEMA7A+ tumors. Thus, we aim to establish novel treatment strategies to improve outcomes for patients with ER+ SEMA7A+ BC. In this paper we investigate the mechanisms by which SEMA7A promotes resistance to endocrine therapy and its potential as a therapeutic target for ER+ BC. Our studies suggest that SEMA7A binds to integrins β1 and β4 and activates AKT mediated pro-survival signaling via its RGD domain. Using syngeneic ER+ models, tumors in were treated with PI3K inhibitors (20mg/kg alpelisib; 10mg/kg GCT-007), alone or in combination with tamoxifen (0.5 mg/100uL peanut oil), which resulted in decreased tumor growth. Tumors were also treated with a combination of an anti-SEMA7A antibody (SmAbH1) (100-250mg/kg) and fulvestrant (83mg/kg), compared to single agents. Our results demonstrate that direct inhibition of SEMA7A via SmAbH1 significantly reduces tumor growth of SEMA7A+ tumors, and the combination with fulvestrant may be even more effective. Our studies suggest that patients with ER+SEMA7A+ tumors should be candidates for PI3K-targeted therapies or anti-SEMA7A-based therapy.

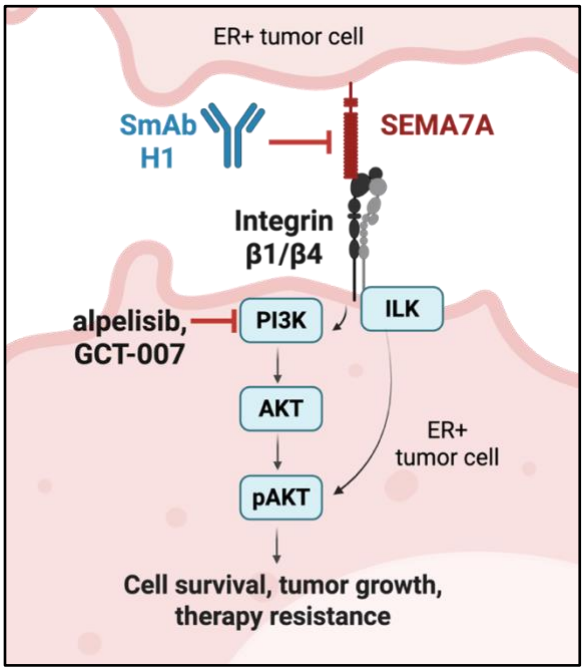

INTRODUCTION

The most prevalent type of breast cancer (BC) is estrogen receptor-positive (ER+), accounting for 70% of all BC diagnoses (1,2). The standard treatment for women with ER+ BC typically involves endocrine therapy, such as the selective ER degrader, fulvestrant, the selective ER modulator, tamoxifen, and aromatase inhibitors such as exemestane and letrozole (2,3). While endocrine therapy is effective in many patients, 22-52% of patients with ER+ BC will experience disease recurrence, depending on lymph node involvement (2,3). Thus, there is an urgent need to improve treatments for patients with ER+ BC. We and others have identified that Semaphorin 7a (SEMA7A), a neuro-endocrine signaling protein (4), is dysregulated in various diseases and cancer types, resulting in poor prognosis (5-13). While numerous studies have investigated the role of SEMA7A in triple-negative breast cancer (TNBC), which lack expression of ER (ER-), progesterone receptor (PR-), and amplification of HER2 (HER2-) (14-19), we have shown that ER can regulate expression of SEMA7A. As such, and have previously analyzed the importance of SEMA7A expression in ER+ BC to show that SEMA7A is expressed in ER+ BC where expression confers resistance to ER targeting therapies including fulvestrant and tamoxifen (2). Our previous studies have also demonstrated mechanisms of therapy resistance activated in ER+ SEMA7A+ tumors that drive reduced sensitivity to the endocrine therapy fulvestrant, including downregulation of ER, activation of pro-survival signaling through Bcl-2, and regulation of markers of drug-resistant stem cells (CD44+/CD24-) (2). We have also shown that long-term estrogen deprivation, such as that induced by endocrine therapies, results in upregulation of SEMA7A and suggest pro-survival signaling as a potential mechanism of resistance(2). In support of this, other studies have shown that pro-survival signaling, such as that mediated by phosphoinositide linked kinase-3 (PI3K), AKT, and other protein kinases, leads to mechanisms of resistance to endocrine therapies (20,21); the contribution of PI3K/AKT to SEMA7A induced phenotypes is still unknown. Therefore, understanding how SEMA7A+ ER+ BCs upregulate pro-survival signaling, and whether these mechanisms could be targetable in SEMA7A+ tumors, will provide insight into treatment strategies for this subset of patients.

27 In previous results, we observed that *SEMA7A* mRNA expression is elevated in 67% of luminal
28 breast cancer cell lines, compared to 50% and 36% in basal A and basal B, respectively (2) and that
29 increased expression results in poor outcomes in all types of breast cancer(2,16). In its immune-related
30 and other roles, SEMA7A is known to bind to two receptors: Plexin C1 and integrin β1 (22), and in
31 models of TNBC we have shown that the pro-tumor roles for SEMA7A are dependent on integrin β1
32 and integrin α6 (14,16). However, in the context of ER+ BC, whether SEMA7A binds integrin receptors
33 remains unknown. Known downstream targets of integrins are those involved in cell adhesion and cell
34 survival, including the PI3K/AKT pathway. In support of a role for SEMA7A- and integrin-mediated
35 activation of the PI3K pathway, studies in TNBC show activation of this pro-survival pathway (15). We
36 have also shown that ER+SEMA7A+ tumors are sensitive to a non-selective PI3K inhibitor (LY294002)
37 that is not utilized clinically. Clinical trials have also shown efficacy of alpelisib or alpelisib plus
38 fulvestrant in PIK3CA-mutated ER+ breast cancer (23,24). Therefore, analysis of clinically relevant
39 PI3K targeted therapies could provide insight into treatment options for patients with SEMA7A+ BC
40 (2,25).
41 Constitutively active PI3K signaling can lead to worse patient prognosis and multidrug
42 resistance, including fulvestrant resistance (20,26,27). We therefore sought to investigate the hypothesis
43 that PI3K inhibitors could be effective for ER+SEMA7A+ BC. In our results presented herein, we show
44 that breast cancer progression is increased in women with ER+SEMA7A+BC, resulting in poor
45 prognosis and highlighting the need to identify additional treatment options. Mechanistically, we show
46 for the first time that SEMA7A binds to integrin β1 and β4, in ER+ breast cancer cells and activates
47 PI3K signaling as well as other phospho-signaling pathways related to cell survival in an integrin-
48 dependent manner. Integrins can activate AKT directly through Integrin-linked kinase (ILK)
49 phosphorylation of AKT at serine 473 (28) and we have previously published that inhibitors of PI3K,
50 ILK, and/or integrins can reduce SEMA7A-mediated activation of pAKT (29); however, integrin and
51 ILK inhibitors are not clinically available, so we explored the effect of PI3K inhibitors in ER+

52 SEMA7A+ tumors. We reveal a partial reversal of endocrine therapy resistance in ER+SEMA7A+
53 models of breast cancer by PI3K inhibition. Further, we tested a novel anti-SEMA7A monoclonal
54 antibody for specifically reducing tumor growth in mice harboring SEMA7A+ tumors, both as a single
55 agent and combined with fulvestrant. Collectively, our results support targeting of SEMA7A, both
56 directly and indirectly through PI3K inhibition, as novel therapeutic strategies to improve patient
57 outcomes in ER+SEMA7A+BC.
58

59 **MATERIALS & METHODS**

60 **Cell Culture:**

61 MCF7 cells were obtained from K. Horwitz (University of Colorado Anschutz Medical Campus). ZR75-
62 1 cells were obtained from the University of Colorado Cancer Center Cell Technologies Shared
63 Resource (CTSR). TC11 cells were obtained from L. Schuler (University of Wisconsin School of
64 Veterinary Medicine). SSM2 cells were obtained from A. Borowsky (University of California Davis).
65 Cell lines were validated by fingerprinting analysis at the University of Colorado Anschutz/Barbara
66 Davis Center Molecular Biology Core. Cells were routinely tested for mycoplasma contamination
67 throughout the studies described herein with Lonza MycLonza MycoAlert PLUS (Walkersville, MD);
68 last tested 3-24-2025. Cells were cultured at 37°C and 5% CO2. MCF7 were grown in MEM with 5%
69 heat-inactivated fetal bovine serum (FBS; Peak Serum PS-FB3, Colorado USA) and 1%
70 penicillin/streptomycin (P/S; ThermoFisher Scientific). TC11 and ZR75-1 were grown in RMPI 1640
71 with 10% heat-inactivated FBS and 1% P/S. SSM2 were grown in DMEM/F12 and supplemented with
72 10% FBS, 1% L-glutamine, 1% P/S. 50 μM 2-mercaptoethanol, 0.3 μM hydrocortisone, 5 μg/ml insulin
73 and 10 ng/ml transferrin. Experiments were performed with cells below passage 30. For exogenous
74 SEMA7A treatments, recombinant SEMA7A (rSEMA7A) was purified from SEMA7A-Fc expressing
75 MDA-MB-231 cells in collaboration with the University of Colorado Cancer Center CTSR (14,30).

76 **Transductions:**

77 MCF7-SEMA7A Overexpressing (OE) and MCF7 empty vector (EV) control cell populations were
78 generated by lentiviral transductions with pLX304-Blast-V5 vectors; CMV-driven, V5-tagged full-
79 length Semaphorin 7a cDNA (666 aa) or empty vector, respectively, and selected for using blasticidin at
80 5 µg/mL (Dana Farber Cancer Institute & CU Anschutz Functional Genomics Core). TC11-control and
81 TC11-SEMA7A knockdown cell lines were generated via lentiviral transduction with pLKO-
82 shNonTargeting-puro, and pLKO-shSEMA7A-038 (KD#1) and pLKO-shSEMA7A-040 (KD#2),
83 respectively, and selected for using puromycin at 2 µg/mL. SEMA7A expression was validated via
84 western blot analysis for all transduced cell lines.

85 **Cell Viability Assays:**

86 Cells were plated in a 96-well (1,000 cells/well), 24-well (100,000 cells/well), 12-well (200,000
87 cells/well) or 6-well (500,000 cells/well) plate in triplicate and allowed to adhere at 37°C for 24 hours.
88 After 24 hours, the cells were treated with vehicle or drug as follows: Fulvestrant and 4-
89 hydroxytamoxifen were purchased from Millipore Sigma (Cat#129453-61-8 and Cat#68392-35-8, St.
90 Louis, MO). For *in vitro* assays, fulvestrant and 4-hydroxytamoxifen treatments were at a final
91 concentration of 8 nM and 5 µM in DMSO, respectively. Alpelisib (BYL719) was purchased from
92 SelleckChem (Cat# S2814) and used at 0.5-1 µM in DMSO, as determined by our dose response and the
93 literature (31). GCT-007 was obtained via collaboration with Global Cancer Technology (San Diego,
94 CA) and used at 0.1-0.5 µM in DMSO as determined by our dose response. Anti-Semaphorin 7a
95 monoclonal antibody; clone H1 (SmAbH1) was obtained from the University of Colorado Cancer
96 Center CTSR. SmAbH1 or Mouse IgG1 (Bio X Cell; Cat# BP0083) was used at 1 µM in PBS as
97 determined by our dose response and the literature (29,32,33). Percent confluence was determined via
98 formalin fixation and 0.1% crystal violet staining and analyzed via ImageJ analysis. Data are normalized
99 to control condition for each treatment. Experiments were performed in biological and technical
100 triplicates and statistics were measured via repeated-measures two-way ANOVA with multiple
101 comparisons.

102 **Drug Titration Studies**:

103 5,000 SEMA7A overexpressing or empty vector control MCF7 cells, or 10,000 TC11 shCtrl or
104 shSEMA7A cells, were seeded per well in a 96-well plate and allowed to adhere overnight. Vehicle or
105 increasing concentrations of drug were added. Growth was assessed using 0.1% crystal violet staining
106 after 24 hours of treatment. To calculate IC50 values, cell viability data for a range of concentrations
107 (minimum 6-points data curve) for each drug was plotted as a dose-response curve in GraphPad Prism
108 and analyzed using nonlinear regression three-parameters curve fit model of log(inhibitor) vs. response.
109 Experiments were performed in triplicate and two-tailed, unpaired t-test was performed on each IC50
110 value in triplicate experiments.

111 **Co-immunoprecipitation**:

112 Pierce Classic Magnetic IP/Co-IP Kit (ThermoFisher; Cat# 88804) and User Guide/CoIP Protocol
113 (Pierce Biotechnologies) was used to perform all CoIP experiments. Cells were cultured normally to
114 optimal confluence in T75 flasks. For RGDS experiments, RGDS peptide (Tocris Bioscience; Cat#3498,
115 50uM in milliQ H_2O) or control (milliQ H_2O) was added to culture media for 1 hour prior to making cell
116 lysates. Lysates were made using IP lysis/wash buffer and incubated on ice for 15 min followed by
117 centrifugation. Protein concentration of lysates was quantified using Qubit Protein Broad Range Assay
118 Kit (ThermoFisher; Cat# A50668). Per sample, 1.0 mg of lysate was pre-incubated with 30 uL IP
119 antibody: mouse IgG or SEMA7A (Santa Cruz; Sc-374432) and rocked overnight at 4°C. Per sample,
120 25µl of Pierce Protein A/G magnetic beads were washed and incubated with the antibody-lysate solution
121 and rocked for 1 hour at room temperature. Using a magnet, supernatant was removed, and the beads
122 were washed with lysis buffer three times. Beads were then eluted with Pierce Elution Buffer, and 10uL
123 (pH) Neutralization Buffer was added per sample. Non-reducing Lane Marker Sample Buffer (5X,
124 Pierce) was used as loading buffer for immunoblots following CoIP elution.

125 **Immunoblotting**:

126 Protein extracts were prepared from cell lines by lysing cells in RIPA with EDTA (Thermo Fisher; Cat#
127 J61529.AP) containing PhosSTOP phosphatase inhibitor (Roche; Cat# 4906837001), and complete
128 protease inhibitor (Roche; Cat# 11697498001). Protein concentration of lysates was determined using

129 Qubit Broad Range Protein Assay Kit (ThermoFisher; Cat# A50668). 30μg of total protein in Laemmli
130 protein sample buffer was heated for 10 minutes. Lysates were run on SDS-Page gels and transferred
131 onto methanol-activated PVDF membranes using the Trans-Blot Turbo Transfer System (Bio-Rad).
132 Membranes were blocked with 5% bovine serum albumin and probed with the following primary
133 antibodies according to manufacturer recommendation: SEMA7A (Santa Cruz; Cat#Sc-374432), pAKT
134 S473 (Cell Signaling; Cat# 4060), total AKT (Cell Signaling; Cat#2920), Integrin β4 (Cell Signaling;
135 Cat#14803), Integrin β1 (Cell Signaling; Cat#34971), ERα (AbCam; Cat#16660), α-tubulin (Cell
136 Signaling; Cat +#9099S) and GAPDH (Biolegend; Cat# 607902). Membranes were washed with 1X
137 Tris-buffered saline with Tween 20, incubated with a goat anti-rabbit HRP secondary antibody (Abcam;
138 Cat# 6721), and developed with enhanced luminescence detection system (Thermo Fisher; Cat# 32106)
139 on the Licor Odyssey. Densitometric O.D. values of three biological replicates were obtained using
140 ImageJ(34) and normalized to the loading control GAPDH or α-tubulin, and normalized to the first
141 sample.

142 **Animal Experiments:**

143 Power calculations based on pilot studies were utilized to determine the number of animals per group.
144 Tumors were measured using digital calipers every 2–3 days with the observer blinded to treatment
145 group, and tumor volume was calculated as (L × W × W × 0.5). Tumors were harvested at designated
146 study endpoints (Maximum tumor volume = 1000mm^3). Mammary glands with intact tumor, axial
147 lymph nodes and lungs were harvested, formalin fixed, and paraffin embedded for
148 immunohistochemical analysis. All animal studies were performed under the approval of the UC
149 Anschutz Medical Campus Institutional Animal Care and Use Committee. Beeswax estrogen (E2) and
150 sham pellets were generated and administered based on previous literature (35). For the study that
151 combined fulvestrant and rSmAbH1-P, tumors were harvested and detached from the mammary gland;
152 photographs were taken next to ruler and scaled to 1cm scale bar.

153 MCF7 Model: MCF7 is a well-known human ER+ cell line used to study breast cancer, thus it was an
154 appropriate model to initiate our studies. 2,500,000 SEMA7A overexpressing or control MCF7 cells
155 were injected into the #4 mammary fat pads of 6–8-week-old female NCG mice (Cat# CRL572, Charles
156 River, Wilmington, MA). For drug treatment studies, fulvestrant dosing began when average tumor
157 volume reached ~100mm^3. At day 37, animals were randomized to treatment into size-matched groups
158 to receive either vehicle or PI3K inhibitor (alpelisib or GCT-007) daily.
159 TC11 Model: TC11 is a syngeneic ER+ murine model which we chose to use because it provides the
160 context of an intact immune system, and there are limited other ER+ mouse models. TC11 also
161 expresses endogenous SEMA7A, making it a relevant model for our research. 200,000 TC11 cells (wild
162 type, shCtrl or shSEMA7A #2) were injected into the bilateral #4 mammary fat pads of 6–8-week-old
163 female FVB/N mice (FVB/NCrl, Cat# CRL207, Charles River, Wilmington, MA). Mice were
164 randomized to treatment into size-matched groups at average tumor volume ~50-100mm^3. For the
165 estrogen/sham pilot study, mice were randomized to groups receiving E2 or sham pellets two days prior
166 to tumor injections.
167 SSM2 Model: SSM2 is another syngeneic ER+ murine model which we chose to use because it provides
168 the context of an intact immune system, and there are limited other ER+ mouse models. SSM2 also
169 expresses endogenous SEMA7A, making it a relevant model for our research. 1,000,000 SSM2 tumor
170 cells were injected into the #4 mammary fat pads of 6–8-week-old female 129 Sv-E mice (129 Sv-E,
171 Cat# CRL287, Charles River, Wilmington, MA). Mice were randomized to treatment into size-matched
172 groups at average tumor volume ~50mm^3.
173 Treatments: Fulvestrant was administered as follows: 2.5 mg in 90% sesame oil and 10% ethanol,
174 injected subcutaneously every 5 days. This dose is equivalent to approximately 83 mg/kg per mouse.
175 Using the FDA Dosing Guidance for Industry: Conversion of Animal Doses to Human Equivalent
176 Doses, equivalent to 6.7mg/kg in humans (2). Tamoxifen was given using the following dosing regimen:
177 0.5 mg/100uL peanut oil per mouse, via intraperitoneal (IP) injection every 3rd day (36). Alpelisib was
178 dissolved in 1% Carboxymethyl cellulose solution + 0.5% Tween 80 and administered via oral gavage at

179 20 mg/kg daily. GCT-007 was dissolved in 55% 1M NaCl, 30% PEG-400, 7.5% Solutol-HS + 7.5% N-
180 Methyl-2-pyrrolidone and administered via oral gavage at 10 mg/kg daily. SmAbH1/rSmAbH1 or
181 Mouse IgG1 (Bio X Cell; Cat# BP0083) was given in sterile PBS at 100-250 µg per 100µL PBS every
182 other day via IP injection (32,33).

183 **Immunohistochemistry:**

184 Tissue collected from the *in vivo* study endpoints as described above, was formalin-fixed and paraffin-
185 embedded. Tissue was stained with Hematoxylin and Eosin. Four-µm sections were pretreated with 10X
186 Dako Target Retrieval System. Slides were prepared in a Dako Autostainer with primary antibody
187 (Integrin β4: Cell Signaling Cat#14803, SEMA7A AbCam Cat # ab255602, 9EG7/CD29: BD
188 Pharmingen rat-anti-mouse CD29 clone 9EG7 Cat# 550531), followed by EnVision+ HRP Rabbit
189 (Agilent Technologies cat# K4003) antibody for 30 mins. For 9EG7 staining, rat-on-mouse HRP
190 polymer detection kit (Biocare cat# RT517H) was used for secondary. The tissue was incubated with
191 chromogen 3,3'diaminobenzidine (Vector Labs catalog #SK-4105) for 10 minutes, and then the tissue
192 was counter-stained with hematoxylin for 1 minute (Vector Labs catalog #H-3401-500). Stained images
193 were acquired using an Olympus Fluorescent Microscope IX83. Quantification was performed using
194 Cell Sense Analysis.

195 **ELISA:**

196 ELISA Buffer Kit (Thermo Cat #CNB0011) was used to perform an indirect ELISA where the plate was
197 coated with SEMA7A protein and probed with serial dilution concentrations of rSmAbH1-P to
198 determine binding specificity. A 96-well plate was pre-coated with 5ug/well of purified SEMA7A
199 (50ug/mL) protein in Coating Buffer A and incubated at 4 degrees overnight. Plate was washed with 1X
200 wash buffer and then probed with primary antibody (rSmAbH1-P) at serial dilution concentrations, from
201 20 to 0 ug/mL, and incubated at 4 degrees overnight. Plate was washed with 1X wash buffer three times
202 and then probed with secondary antibody (Goat anti-mouse IgG-HRP; Abcam Cat#ab97040) for 30

203 minutes at room temperature. Plate was washed three times with 1X wash buffer and absorbance at
204 425nm was read on plate reader.

205 **Data Mining Analysis:**

206 Kaplan Meir Plotter(37) was used to assess overall survival (OS), distant metastasis-free survival
207 (DMFS), and post-progression survival (PPS) data for BC patients in the ER+ dataset, and patients in
208 the ER+ dataset who received endocrine therapy (tamoxifen or fulvestrant). SEMA7A was queried and
209 stratified into high and low-expression groups using the auto-select best cutoff level function. The
210 generated data, plots, hazard ratio (HR), and LogRank P value were downloaded from KMplotter.com.
211 TCGA Human Data Analysis: We analyzed The Cancer Genome Atlas (TCGA) Breast Cancer study for
212 the mRNA expression of Semaphorin 7a (*SEMA7A),* integrin β1 *(ITGB1), and* integrin β4 *(ITGB4)*
213 collected from patient samples processed by RNAseq – IlluminaHiSeq. Gene expression analysis was
214 performed using the Xena Functional Genomics Explorer(38). The log2(norm_count+1) value for
215 mRNA expression was used to graph correlations between SEMA7A and the other genes in the TCGA
216 Breast Cancer dataset. Each data was analyzed using Pearson's correlation (rho) and p-values are
217 indicated on each plot.

218 **BioSpa Assay:**

219 500 MCF7 cells per well were plated in 96 well plates and incubated overnight to allow for adherence.
220 Cells were then treated with 1μM IgG1 or 1μM SmAbH1 and immediately placed in a BioSpa Live Cell
221 Imager (Agilent) for 4 days, with images of each well being taken every 4 h, at ×10 magnification. The
222 cell count of each well was measured via brightfield count in the BioSpa Software.

223 **Reverse Phase Protein Array (RPPA):**

224 For cell lysates (RPPA-1), MCF7 Empty Vector control or SEMA7A Overexpressing cells were
225 cultured, each in quadruplicate, in a 10cm dish for 72 h. After washing cells with PBS, lysates were
226 generated using RPPA Lysis Buffer (Baylor College of Medicine Antibody-Based Proteomics Core) and
227 frozen at -20°C. For tumor RPPA (RPPA-2), tumors were harvested and flash-frozen in liquid nitrogen
228 at necropsy and stored at -80°C. Lysates/tumors were shipped on dry ice to the Baylor College of

229 Medicine (BCM) Antibody-Based Proteomics Core (Houston, TX). Subsequent RPPA was performed
230 by the core facility as outlined here (https://www.bcm.edu/academic-centers/dan-l-duncan-
231 comprehensive-cancer-center/research/cancer-center-shared-resources/antibody-based-
232 proteomics/protocols-workflow) (39). Normalized fold change for each antibody was calculated by
233 (each signal value/AVG value of controls) and is depicted as log2(normalized fold change. Significance
234 was determined by performing an unpaired two-tailed t-test between the fold change values for each
235 antibody. Each sample was run in technical triplicates and n=4 samples per group. Samples with a
236 Coefficient of Variation >25% for technical triplicates were excluded from further analysis. Pathway
237 analysis was done using Gene Ontology Pathway Analysis.

238 **Protein Ribbon Structures:**

239 The protein structure of SEMA7A was analyzed in PyMOL with an academic research license. Ribbon
240 structure (purple) was created and modified to highlight the RGD motif (orange) and the antibody-
241 binding site (green) in PyMOL.

242 **Synergy Scores:**

243 Bliss Synergy scores for two-drug combination treatments were calculated using Synergyfinder.org;
244 scores ≤ -10 are considered antagonistic, between -10 and 10 are considered additive, and a score ≥ 10 is
245 considered synergistic (40). Further details on the methods used can be found at
246 https://synergyfinder.fimm.fi/synergy/synfin_docs/.

247 **Novel drug treatments:**

248 SmAbH1 (hybridoma): Mice were injected with SEMA7A protein and KLH peptide to enhance
249 immune response. B cells from mouse spleens were fused with myeloma cells to create a hybridoma;
250 positive hybridoma clones were selected and monoclonal antibodies were harvested. SmAbH1 Antibody
251 binds to amino acids 381-392 of SEMA7A (green; SFigure 1G) (29).

252 rSmAbH1 (recombinant): The ExpiCHO-S expression system (Gibco) was used for the production of
253 recombinant antibodies according to the manufacturer's protocol. After the 12 days of expression, the
254 culture media were harvested by centrifugation, filtered through a 0.2-micron filter, and underwent

255 affinity chromatography using MabSelect PrismA resin and the AKTA pure FPLC instrument for
256 purification of recombinant monoclonal antibody.
257 GCT-007: GCT-007 is a pan PI3K inhibitor and was provided to us for these studies by Global Cancer
258 Technology. (16776 Bernardo Center Drive #203, San Diego, CA 92128).

259 **Statistical Analysis:**

260 All quantitative and statistical analysis was performed using GraphPad Prism (Version 10.3.1), and the
261 methods of tests are labeled in the figure legends. The statistical tests used in this paper include unpaired
262 two-tailed t-test, Pearson's correlation, and ordinary one-way ANOVA with Tukey's multiple
263 comparisons test. All p-values were measured under two-tailed conditions. Significance was determined
264 by a p-value less than 0.05. *$p<0.05$, **$p<0.01$, ***$p<0.001$ ****$p<0.0001$.

265 **Data Availability:**

266 The data generated in this study are available upon request from the corresponding author.

267

268 **RESULTS**

269 **SEMA7A is expressed in ER+ breast cancer and associated with decreased 5-year patient survival.**

270 To test our hypothesis that SEMA7A predicts decreased response to therapy, and therefore poor
271 prognosis, we used Kaplan-Meier Plotter(37) to examine 5-year survival for ER+ BC patients with high
272 versus low tumor *SEMA7A* mRNA expression (Figure 1A-C). The probability of overall survival (OS)
273 was significantly decreased for patients with high *SEMA7A* expression (Figure 1A), as well as distant
274 metastasis-free survival (DMFS) (Figure 1B) and post-progression survival (PPS) (Figure 1C). Further,
275 relapse-free survival (RFS) (Figure 1D) and DMFS (Figure 1E) were decreased in ER+ BC patients with
276 high *SEMA7A* expression who received endocrine therapy.

277 **SEMA7A activates AKT signaling and binds to Integrins β1 and β4 via RGD in ER+ tumor cells.**

278 To investigate differential protein and phospho-protein expression in ER+ MCF7 breast cancer
279 cells transduced with an empty vector (EV) or SEMA7A overexpression (OE) vector, we utilized a
280 reverse phase protein array (RPPA-1) (41). We confirmed SEMA7A overexpression via western blot

281 prior to submission of lysates for RPPA (SFigure 1A). Using the data obtained from RPPA-1 we
282 performed Gene Ontology (GO) Analysis to identify upregulated pathways in the SEMA7A OE lysates
283 compared to EV; we observed that signaling related to cell survival, including AKT, mTOR, and
284 integrin signaling, was upregulated in SEMA7A OE cells (Figure 2A). Specifically, the RPPA data
285 suggest that overexpression of SEMA7A leads to increased integrins β1 and β4 as well as phospho-AKT
286 (pAKT) at serine 473 (S473) (Figure 2B). The RPPA also show that integrin-linked kinase, which can
287 activate AKT through S473 phosphorylation (42), the anti-apoptotic protein Bcl-2, and downstream
288 targets of AKT, such as p-P70S6K (S371), were all increased in SEMA7A OE lysates (Figure 2B).
289 Phospho-mTOR(S2448), which is also a downstream target of AKT, was also increased, but not with
290 statistical significance (p=0.0564)(Figure 2B). To validate that SEMA7A activates AKT signaling
291 through pAKT (S473) in ER+ breast cancer cells, we validated pAKT (S473) and total AKT using
292 immunoblot analysis on MCF7 EV and SEMA7A OE cells, or WT MCF7 treated with purified
293 SEMA7A (rSEMA7A); the pAKT to AKT ratio was significantly higher in SEMA7A OE cells
294 compared to EV and rSEMA7A-treated cells compared to controls (SFigure 1B-C). Expression of
295 *ITGB1* and *ITGB4* mRNA also weakly correlated with *SEMA7A* expression in the TCGA Breast Cancer
296 Dataset (n=1247) (SFigure 1D-E). To investigate integrin β1 and β4 as binding partners for SEMA7A in
297 ER+ breast cancer cells, we performed co-immunoprecipitation (CoIP) using a SEMA7A specific
298 antibody to bind the protein and its binding partner(s). After CoIP, western blotting revealed binding of
299 both integrin β1 and β4 to SEMA7A, which was higher in SEMA7A OE cells compared to controls
300 (Figure 2C, SFigure 1G: CoIP input and unbound controls). To investigate whether SEMA7A binds to
301 integrins via its RGD (Arg-Gly-Asp) motif (SFigure 1F), which is known to facilitate integrin binding
302 (43), we conducted CoIP using MCF7 SEMA7A OE lysates treated with PBS or RGDS (Arg-Gly-Asp-
303 Ser) peptide, which inhibits RGD-integrin binding. Our results indicate that binding of SEMA7A to
304 integrin β1 and β4 was significantly reduced by the RGDS peptide (Figure 2D, SFigure 1H: CoIP input

305 and unbound contorls). These results were validated in an additional human ER+ breast cancer cell line,
306 ZR75-1 (SFigure 1I).

307 **SEMA7A-mediated activation of AKT is dependent on RGD binding in ER+ tumor cells.**

308 Based on our results showing increased pAKT (S473) in SEMA7A OE MCF7, we validated our
309 results in a syngeneic ER+ cell line. We obtained TC11 and SSM2 cells, which are ER+ mouse
310 mammary tumor cell lines (44,45)(generous gifts from Linda Schuler and Alexander Borowsky), and
311 validated ERα expression compared to MCF7 (SFigure 2A). We also compared SEMA7A expression in
312 the two cell lines to reveal that TC11 cells express slightly higher endogenous SEMA7A (SFigure 2B).
313 To determine whether SEMA7A was necessary to drive pAKT in the TC11 cell line, we compared cell
314 lines stably transduced with shCtrl and shSEMA7A lentiviral vectors (shSEMA7A KD#1 and KD#2).
315 We confirmed SEMA7A expression was decreased in both KD vectors, with a larger decrease in KD#2
316 (SFigure 2C). As expected, knockdown of SEMA7A decreased pAKT levels, and the ratio of pAKT to
317 AKT was decreased in a SEMA7A-dependent manner (Figure 3A). Additionally, we show that
318 recombinant SEMA7A (rSEMA7A) or conditioned media from SEMA7A OE cells rescued the decrease
319 in pAKT observed in the KD cells (Figure 3B). To further define whether AKT activation by SEMA7A
320 occurs via SEMA7A-integrin binding, we treated TC11 cells with rSEMA7A, RGDS peptide or both,
321 and measured pAKT/AKT expression (Figure 3C). Although the RGDS peptide alone inhibited pAKT
322 levels, our results also show that rSEMA7A increased pAKT, and this effect was inhibited by the RGDS
323 peptide (Figure 3C). We observed similar results with the RGDS in two additional ER+ cell lines,
324 MCF7 and ZR751 (SFigure 2D-E).

325 **SEMA7A+ tumor growth is inhibited by combination treatment with endocrine therapy and PI3K**
326 **inhibitors.**

327 Since there are no clinically available integrin or ILK inhibitors, we investigated other
328 therapeutic strategies to inhibit SEMA7A-mediated signaling. Increased pAKT levels in SEMA7A-
329 expressing cells suggest a potential increase in PI3K signaling activity (46). Thus, we hypothesized that
330 SEMA7A+ ER+ BC cells would exhibit increased sensitivity to treatment with PI3K inhibitors (PI3Ki).

331 To test this hypothesis, we determined the 50% inhibitory concentration (IC50) for alpelisib (p110α
332 inhibitor) and GCT-007 (pan-PI3K inhibitor in development for treatment in glioblastoma and breast
333 cancer(47)) in MCF7 EV and SEMA7A OE cells (SFigure 3A-B). The IC50 of alpelisib and GCT-007
334 in SEMA7A OE cells was lower, suggesting increased susceptibility to PI3Ki in SEMA7A-expressing
335 tumor cells. We also examined sensitivity to PI3Ki in TC11 shSEMA7A #2 KD cells compared to
336 controls (SFigure 3C-D). In support of our hypothesis, cell viability assays revealed that inhibition by
337 both alpelisib and GCT-007 is greater in SEMA7A OE cells, compared to controls (SFigure 3E). We
338 also confirmed that pAKT expression is reduced by both PI3Ki treatments in MCF7 and TC11 (SFigure
339 3F-G) cells.

340 Since PI3K inhibition is utilized clinically in conjunction with endocrine therapy for ER+ breast
341 cancers, we aimed to evaluate whether a combination of endocrine therapy and PI3K inhibition (PI3Ki)
342 would be more effective than either treatment alone in SEMA7A-expressing tumors. Based on previous
343 literature (2) and our IC50 curves (SFigure 3A-D; SFigure 4A-B), we treated ER+ TC11 cells with
344 fulvestrant, alpelisib, or the combination and measured cell viability to reveal that fulvestrant alone had
345 minimal effect, while single-agent alpelisib and GCT-007 resulted in a moderate reduction in cell
346 viability, and the combination treatments were the most effective (Figure 4A-B). Similar results were
347 observed with the combination of fulvestrant plus alpelisib or GCT-007 in another ER+ cell line, ZR75-
348 1 (SFigure 4C-D). Notably, TC11 tumor cells are reported to exhibit resistance to tamoxifen (44).
349 Therefore, we also tested the combination of tamoxifen and each PI3Ki in TC11 cells; our findings
350 reveal that tamoxifen alone has minimal effect, whereas the combination significantly reduced cell
351 viability compared to control, to a greater extent than either single agent (Figure 4C-D). Following *in*
352 *vitro* synergy assays, Bliss synergy scores were calculated for the treatment combinations of fulvestrant
353 (Figure 4E-F) and tamoxifen (Figure 4G-H) with PI3K inhibitors. Synergy scores between 0 and 10
354 indicate an additive effect, while scores above 10 indicate synergy between two treatments, and we
355 observed synergy with fulvestrant/alpelisib (Score = 11.3), tamoxifen/alpelisib (Score = 14.61) and
356 tamoxifen/GCT-007 (Score = 16.33), and an additive effect with fulvestrant/GCT-007 (Score = 3.52)

357 (40). To evaluate the combination of endocrine therapy and PI3K inhibition *in vivo*, MCF7 SEMA7A
358 OE tumor-bearing NCG mice were treated with fulvestrant alone or in combination with alpelisib or
359 GCT-007, resulting in a greater reduction of tumor growth with the combination treatments (SFigure
360 4E-F). We monitored mouse weight and moribound criteria and observed no evidence of toxicities with
361 either PI3K inhibitor based on these criteria (SFigure 4G-H). In data from the manufacturer, GCT-007
362 exhibits efficacy in immunocompetent mice using a model of glioblastoma (unpublished observations).
363 Therefore, we tested combination treatments in an ER+ (SFigure 4I), estrogen-responsive (44)(SFigure
364 4J) immune-competent model. TC11 tumor-bearing FVB/N mice were treated with tamoxifen, GCT-
365 007, or the combination; the combination was most effective at inhibiting tumor growth compared to
366 either single agent or controls (Figure 4I). Consistent with the previous study, mouse no evidence of
367 toxicity was observed (SFigure 4K).

368 **Inhibition of SEMA7A using a monoclonal antibody (SmAbH1) reduces tumor growth and AKT**
369 **signaling in ER+ BC.**

370 We next tested our hypothesis that resistance to endocrine therapy, mediated by SEMA7A (2),
371 could be reversed by direct targeting of SEMA7A using our novel anti-SEMA7A monoclonal antibody
372 (SmAbH1) that we have previously shown to have efficacy in ER-negative models of breast
373 cancer(32,33). Our *in vitro* BioSpa live imaging assay results show that cell viability is reduced by
374 SmAbH1 over time in MCF7 SEMA7A OE cells, but not in EV controls (Figure 5A). The IC50 for
375 SmAbH1 is also lower in SEMA7A OE compared to controls (SFigure 5A), suggesting SmAbH1 is
376 most effective in SEMA7A-expressing cells. Previous studies from our lab have confirmed binding
377 specificity of SmAbH1 to SEMA7A protein via ELISA (29). In contrast, TC11 SEMA7A shSEMA7A
378 KD#2 showed less response to SmAbH1 compared to TC11 shCtrl cells *in vitro* (Figure 5B). Our
379 previous studies suggest that SmAbH1 is not efficacious in immune-compromised hosts (32). Thus, we
380 evaluated SmAbH1 in the TC11 model *in vivo* (SFigure 5B-D). We observed inhibition of tumor growth
381 in SmAbH1-treated tumors only (SFigure 5B-C). We observed no evidence of toxicity based on mouse
382 weight and moribound criteria (SFigure 5D). We validated these findings in the SSM2/129Sv-E model,

383 an additional ER+ immune-competent model (48) with endogenous SEMA7A expression (SFigure 2B,
384 SFigure 5E). As further evidence of specificity of SmAbH1, we observed that SmAbH1 inhibited tumor
385 growth compared to the IgG control (Figure 5C) and this effect was specific to SEMA7A-expressing
386 shCtrl tumors only (Figure 5C). Similarly, tumor volume calculated at study endpoint and tumor weight
387 were significantly reduced only in the TC11 shCtrl tumors treated with SmAbH1 (Figure 5D-E). To
388 confirm a SEMA7A/integrin-mediated mechanism *in vivo*, we performed IHC staining on control and
389 SmAbH1-treated TC11 tumors (Figure 5F). To look at pAKT levels, we performed RPPA analysis
390 (RPPA-2) of lysates made from IgG-treated and SmAbH1-treated TC11 and SSM2 tumors to reveal
391 decreased expression of pAKT (S473) in SmAbH1-treated tumors (Figure 5G, SFigure 5F). Further,
392 quantification of tumor IHC staining showed that activated integrin β1 (via 9EG7 staining), integrin β4,
393 and SEMA7A protein expression were reduced in the SmAbH1-treated group (Figure 5H-J, SFigure 5G:
394 secondary-only IHC controls, SFigure 5H-J: n=5 per group).

395 **Combination treatment with fulvestrant and SmAbH1 reduces SEMA7A+ ER+ tumor growth.**

396 To test the hypothesis that the combination of SmAbH1 and fulvestrant may benefit patients, we
397 tested cell viability in TC11 and MCF7 cell lines. TC11 shCtrl cell viability was inhibited by SmAbH1
398 alone, and even more so by combination of fulvestrant and SmAbH1, whereas TC11 shSEMA7A KD#2
399 viability was not affected (Figure 6A). Further, treatment of MCF7 EV and SEMA7A OE cells with
400 fulvestrant, SmAbH1, or the combination showed that SEMA7A OE cells respond positively to
401 SmAbH1 as a single agent and even more robustly to the combination of fulvestrant and SmAbH1,
402 while control cells do not (SFigure 6A). Additionally, EV cells exhibit a moderate response to
403 fulvestrant alone, while SEMA7A OE cells do not (SFigure 6A). These results were validated in SSM2
404 and ZR75-1 cells (SFigure 6B-C). In contrast, TC11 shSEMA7A cells displayed increased sensitivity to
405 fulvestrant alone *in vitro* (Figure 6A), suggesting that loss of SEMA7A may re-sensitize TC11 tumor
406 cells to fulvestrant. We also calculated synergy scores for fulvestrant in combination with SmAbH1 in
407 TC11 cells (Figure 6B). SmAbH1 with fulvestrant resulted in a synergistic score (Bliss score>10), while
408 SmAbH1 with tamoxifen was only slightly additive (Bliss score<10) (SFigure 6D), thus we moved

409 forward with fulvestrant. To test our hypothesis *in vivo,* TC11 shCtrl and shSEMA7A KD#2 tumor cells
410 were implanted into FVB/N mice and groups with Vehicle, IgG1, fulvestrant, SmAbH1, or the
411 combination. Tumor growth of shCtrl tumors was reduced by SmAbH1 and the combination therapy,
412 but not by the IgG or vehicle controls or fulvestrant alone (Figure 6C). Consistent with our hypothesis,
413 growth of TC11 shSEMA7A tumors was not affected by SmAbH1 alone but was reduced by fulvestrant
414 and the combination therapy (Figure 6D). Previous results were obtained with a hybridoma derived
415 SmAbH1. Thus, we also tested a recombinant version of anti-SEMA7A antibody, rSmAbH1, for range
416 of reactivity and specificity via IC50 and ELISA assay (SFigure 6E-F). Synergy results revealed that
417 rSmAbH1-P and fulvestrant are synergistic *in vitro,* similar to what was observed with SmAbH1 and
418 fulvestrant (SFigure 6G). We then repeated the TC11 *in vivo* experiment with rSmAbH1-P and
419 fulvestrant; images of harvested tumors show visibly smaller tumors in the rSmAbH1-P-treated and
420 combination-treated groups compared to controls or fulvestrant alone (Figure 6E). Mouse weights were
421 monitored (SFigure 6H), and a 6-chemistry toxicity panel was run on mouse plasma and showed no
422 differences between rSmAbH1-P-treated treatment and control-treated mice (SFigure 6I-N).

423 **DISCUSSION**

424 Collectively, our results reveal mechanisms of action and therapeutic vulnerabilities of SEMA7A
425 expressing ER+BC. Previous studies implicated integrin β1 as a receptor for SEMA7A on cancer cells
426 and other cell types, our findings suggest that SEMA7A binds to both integrin β1 and β4 in ER+ breast
427 cancer cells (Figure 2). We also provide evidence that the RGD motif within SEMA7A mediates binding
428 to β-integrins. Furthermore, our findings with the RGDS blocking peptide suggest that SEMA7A
429 enhances phosphorylation and activation of AKT specifically through integrins, which were previously
430 shown to undergo conformational changes when bound by an RGD motif leading to intracellular
431 activation of signaling pathways such as PI3K/AKT, ILK, Fak, and MAPK/ERK (49). Our results are
432 consistent with previously results showing that integrin β1 activation of PI3K and MAPK signaling can
433 facilitate endocrine therapy resistance in breast cancer (50); thus blocking this SEMA7A mediated

434 pathway is a potential way to overcome endocrine therapy resistance in patients with ER+BC.
435 Limitations of the current study include that the synthetic RGDS peptide may have also caused non-
436 specific integrin inhibition beyond that attributed to SEMA7A. Further, while the RGD motif in
437 SEMA7A is known, the protein folding structure of SEMA7A when bound versus unbound to integrins
438 remains unknown. Future studies could further investigate this protein interaction through mutations and
439 further structural analyses.

440 Our findings provide premise for treating patients with SEMA7A+ breast cancer with more
441 targeted therapies, including those that target of PI3K and/or directly target SEMA7A. Given our
442 previous studies showing poor relapse-free survival rates in both ER+ and ER- breast cancer patients (2),
443 clinical trials informed by our data stand to impact thousands of patients annually. We observed a
444 correlation between SEMA7A overexpression and increased pAKT (S473) and downstream targets of
445 AKT, suggesting activation of downstream survival signaling by AKT. Since ILK was moderately
446 increased in SEMA7A OE cells and ILK is known to phosphorylate AKT at S473, we suspect
447 involvement of ILK downstream of SEMA7A/integrin signaling. Because there are no clinically
448 available integrin or ILK inhibitors, we suggest that clinically approved PI3K inhibitors be tested to
449 inhibit the SEMA7A-AKT pathway. Clinical use of alpelisib is currently approved for patients with an
450 E545K mutation in *PIK3CA* that causes constitutive activation of the PI3K p110α subunit (24,51).
451 However, we hypothesize that even in the absence of the *PIK3CA* E545K mutation, high SEMA7A
452 expression can cause hyperactivation of PI3K including p110α, thus SEMA7A-expressing tumors may
453 be sensitive to alpelisib (52). GCT-007, a pan-PI3K inhibitor that has shown preclinical efficacy in
454 glioblastoma, is not approved yet for clinical use, but our results suggest it may be efficacious in breast
455 cancer patients as well. Limitations of the clinical applicability of our study include the known toxicities
456 observed in some patients including hyperglycemia, rash, and diarrhea (53), and while we saw no overt
457 toxicities in our mouse studies, the potential toxicities of GCT-007 in humans is unknown. Additionally,
458 while we did not explore direct targeting of AKT future studies could determine that this is another

459 viable option for patients with ER+SEMA7A+BC. Pan-AKT inhibitors such as capivasertib and
460 ipatasertib, mTOR inhibitors such as everolimus, and other PI3K inhibitors such as a p110δ inhibitors
461 (idelalisib) could be explored in our SEMA7A+ER+BC models to optimize available treatment
462 combinations. Moreover, we have published that the Bcl-2 inhibitor venetoclax can slow tumor growth
463 in pre-clinical models, and our RPPA-1 results confirm increased Bcl-2 expression with SEMA7A
464 expression; thus, combination of SmAbH1 and venetoclax should also be explored.

465 Our results suggest that direct inhibition of SEMA7A via our monoclonal antibody, SmAbH1, is
466 a promising therapeutic strategy that should be further investigated with additional pre-clinical studies to
467 enable progression to first in human clinical trials. While the combination of fulvestrant and SmAbH1
468 did reach statistical significance compared to SmAbH1 alone, it is important to note that SmAbH1 did
469 not appear to interfere with fulvestrant, which is utilized clinically for ER+ breast cancers and at study
470 end the tumors were visibly smaller in the combination-treated group. These results suggest that patients
471 will obtain benefit from the addition of SmAbH1 to their current standard of care (continued endocrine
472 therapy) in the recurrent/metastatic setting and that after additional testing SmAbH1 could become a
473 novel front line therapy for ER+BC patients that express SEMA7A. Aside from reduced tumor growth,
474 we also saw that SmAbH1 decreased pAKT (S473) suggesting that SmAbH1 is functionally inhibiting
475 the pathway activated by SEMA7A/integrin interaction. We also performed additional in vivo
476 SmAb/fulvestrant studies with a newly generated recombinant antibody, rSmAbH1-P, which is
477 necessary for humanization and future IND-enabling studies. A limitation of our study is the use of
478 mouse cell lines for the *in vivo* models instead of human cell lines. We deliberately chose the TC11 and
479 SSM2 models to test SmAbH1 because they are immunocompetent and we have recently published that
480 SmAbH1 activates anti-tumor T cell responses by re-activating anti-tumor T cell responses (29).

481 We conclude that inhibition of SEMA7A mediated signaling in breast cancer, both direct and
482 indirect, are promising clinical treatment avenues that should be further investigated particularly in
483 patients with recurrent disease despite endocrine therapies. Furthermore, our previous results suggest
484 that SEMA7A positive tumors will not respond to CDK4/6 inhibition, which is FDA approved for ER+

breast cancer patients. Additionally, our results suggest that patients with ER+ BC may benefit from a diagnostic test that quantifies SEMA7A expression as we have published a threshold of SEMA7A expression by immunostaining fixed tissues that can predict for relapse in a small patient dataset(17). If such a diagnostic existed, patients with SEMA7A+ tumors could receive a SEMA7A-targeted therapy like patients with HER2+ disease that are treated with trastuzumab. Future directions could also include the development and optimization of a minimally invasive SEMA7A-detecting diagnostic (blood) test, which we have initiated. However, further investigation is needed to determine whether SEMA7A levels in tumors correlate with levels in patient serum samples. Cumulatively, our current and previous studies suggest a unique and druggable aspect in the biology of SEMA7A-expressing breast cancers that could transform treatment options for ER+BC.

ACKNOWLEDGEMENTS

- Technical support
    - Lyons Lab: Lyndsey Crump, Lauren Cozzens, Kelsey Kines, Alan Elder, Alex Becks (University of Colorado Anschutz)
    - Sarah Tarullo (Plymouth State University)
    - Porter lab: Weston Porter, Garhett Wyatt (Texas A&M)
- Provided Reagents:
    - Global Cancer Technology
    - Novartis
- Clinical mentor:
    - Virginia Borges (CU Anschutz, UC Health)
- Thesis committee members: Carol Sartorius, Benjamin Bitler, Katherine Fantauzzo, John Tentler, Jennifer Richer, Daniel Sherbenou
- Experimental advice:
    - Michael Oliphant

- NIH/NCATS Colorado CTSA Grant Number TL1 TR002533 to RS
- NIC R01CA282900-01 and R01HD108335-01A1 to TL
- SPARK/REACH Program, NIH: U01HL152405 and OEIDIT/AIA: MA 2021-2028 to TL
- ABN Ohana Gates Grubstake Award to TL
- DOM Outstanding Early Career Scholars Program to TL
- UCCC and DOM ASPIRE to TL
- Men for the Cure PO1 pilot grant to TL
- University of Colorado Cancer Center Support Grant #P30CA046934 to RS
    - Anh Le, Steve Anderson and the University of Colorado Anschutz CTSR (Cell Technologies Shared Resource)
    - University of Colorado Anschutz CPSR (Comparative Pathology Shared Resource)
- Cancer Prevention & Research Institute of Texas Core Facility Support Awards (PR210227, PI: Dean Edwards)
    - Baylor College of Medicine Antibody-Based Proteomics Core
        - Dean Edwards
        - Shixia Huang

REFERENCES

1. ACS. 2024 American Cancer Society: Cancer Facts and Figures 2024. In American Cancer Society <https://www.cancer.org/research/cancer-facts-statistics/all-cancer-facts-figures/2024-cancer-facts-figures.html>.

2. Crump LS, Wyatt GL, Rutherford TR, Richer JK, Porter WW, Lyons TR. Hormonal Regulation of Semaphorin 7a in ER⁺ Breast Cancer Drives Therapeutic Resistance. Cancer Research **2021**;81:187-98

3. Pan H, Gray R, Braybrooke J, Davies C, Taylor C, McGale P*, et al.* 20-Year Risks of Breast-Cancer Recurrence after Stopping Endocrine Therapy at 5 Years. N Engl J Med **2017**;377:1836-46

4. Pasterkamp RJ, Peschon JJ, Spriggs MK, Kolodkin AL. Semaphorin 7A promotes axon outgrowth through integrins and MAPKs. Nature **2003**;424:398-405

540 5. Bao ZZ, Jin Z. Sema3D and Sema7A have distinct expression patterns in chick embryonic
541 development. Dev Dyn **2006**;235:2282-9

542 6. Kohler D, Granja T, Volz J, Koeppen M, Langer HF, Hansmann G*, et al.* Red blood cell-derived
543 semaphorin 7A promotes thrombo-inflammation in myocardial ischemia-reperfusion injury
544 through platelet GPIb. Nat Commun **2020**;11:1315

545 7. Manini I, Ruaro ME, Sgarra R, Bartolini A, Caponnetto F, Ius T*, et al.* Semaphorin-7A on
546 Exosomes: A Promigratory Signal in the Glioma Microenvironment. Cancers (Basel) **2019**;11

547 8. Kinehara Y, Nagatomo I, Koyama S, Ito D, Nojima S, Kurebayashi R*, et al.* Semaphorin 7A
548 promotes EGFR-TKI resistance in EGFR mutant lung adenocarcinoma cells. JCI Insight **2018**;3

549 9. Xie J, Wang H. Semaphorin 7A as a potential immune regulator and promising therapeutic target
550 in rheumatoid arthritis. Arthritis Res Ther **2017**;19:10

551 10. Vaidya B, Patel R, Muth A, Gupta V. Exploitation of Novel Molecular Targets to Treat
552 Idiopathic Pulmonary Fibrosis: A Drug Discovery Perspective. Curr Med Chem **2017**;24:2439-
553 58

554 11. Garcia-Areas R, Libreros S, Simoes M, Castro-Silva C, Gazaniga N, Amat S*, et al.* Suppression
555 of tumor-derived Semaphorin 7A and genetic ablation of host-derived Semaphorin 7A impairs
556 tumor progression in a murine model of advanced breast carcinoma. Int J Oncol **2017**;51:1395-
557 404

558 12. Gutierrez-Franco A, Eixarch H, Costa C, Gil V, Castillo M, Calvo-Barreiro L*, et al.* Semaphorin
559 7A as a Potential Therapeutic Target for Multiple Sclerosis. Mol Neurobiol **2016**

560 13. Roth JM, Kohler D, Schneider M, Granja TF, Rosenberger P. Semaphorin 7A Aggravates
561 Pulmonary Inflammation during Lung Injury. PLoS One **2016**;11:e0146930

562 14. Tarullo SE, Hill RC, Hansen KC, Behbod F, Borges VF, Nelson AC*, et al.* Postpartum breast
563 cancer progression is driven by semaphorin 7a-mediated invasion and survival. Oncogene
564 **2020**;39:2772-85

565 15. Rutherford TR, Elder AM, Lyons TR. Anoikis resistance in mammary epithelial cells is
566 mediated by semaphorin 7a. Cell Death Dis **2021**;12:872

567 16. Black SA, Nelson AC, Gurule NJ, Futscher BW, Lyons TR. Semaphorin 7a exerts pleiotropic
568 effects to promote breast tumor progression. Oncogene **2016**;35:5170-8

569 17. Borges VF, Hu J, Young C, Maggard J, Parris HJ, Gao D*, et al.* Semaphorin 7a is a biomarker
570 for recurrence in postpartum breast cancer. npj Breast Cancer **2020**;6:56

571 18. Elder AM, Tamburini BAJ, Crump LS, Black SA, Wessells VM, Schedin PJ*, et al.* Semaphorin
572 7A Promotes Macrophage-Mediated Lymphatic Remodeling during Postpartum Mammary
573 Gland Involution and in Breast Cancer. Cancer Res **2018**;78:6473-85

574 19. Kines KaF, Heather and Elder, Alan and Cozzens, Lauren and Strugar, Zachary and Porter,
575 Weston and Borges, Virginia and Lyons, Traci, . Aging-Induced Semaphorin 7a Promotes
576 Tgfβ1-Mediated Cell Plasticity and Breast Tumor Metastases. **2024**

577 20. Burris HA, 3rd. Overcoming acquired resistance to anticancer therapy: focus on the
578 PI3K/AKT/mTOR pathway. Cancer Chemother Pharmacol **2013**;71:829-42

579 21. Truong TH, Benner EA, Hagen KM, Temiz NA, Kerkvliet CP, Wang Y*, et al.* PELP1/SRC-3-
580 dependent regulation of metabolic PFKFB kinases drives therapy resistant ER+ breast cancer.
581 Oncogene **2021**;40:4384-97

582 22. Suzuki K, Kumanogoh A, Kikutani H. Semaphorins and their receptors in immune cell
583 interactions. Nat Immunol **2008**;9:17-23

584 23. Andre F, Ciruelos EM, Juric D, Loibl S, Campone M, Mayer IA*, et al.* Alpelisib plus fulvestrant
585 for PIK3CA-mutated, hormone receptor-positive, human epidermal growth factor receptor-2-
586 negative advanced breast cancer: final overall survival results from SOLAR-1. Ann Oncol
587 **2021**;32:208-17

588 24. André F, Ciruelos E, Rubovszky G, Campone M, Loibl S, Rugo HS*, et al.* Alpelisib for
589 PIK3CA-mutated, hormone receptor–positive advanced breast cancer. New England Journal of
590 Medicine **2019**;380:1929-40

591 25. Duarte A, Silveira GG, Soave DF, Costa JPO, Silva AR. The Role of the LY294002 - A Non-
592 Selective Inhibitor of Phosphatidylinositol 3-Kinase (PI3K) Pathway- in Cell Survival and
593 Proliferation in Cell Line SCC-25. Asian Pac J Cancer Prev **2019**;20:3377-83

594 26. Yang SX, Polley E, Lipkowitz S. New insights on PI3K/AKT pathway alterations and clinical
595 outcomes in breast cancer. Cancer Treat Rev **2016**;45:87-96

596 27. Bostner J, Karlsson E, Pandiyan MJ, Westman H, Skoog L, Fornander T*, et al.* Activation of
597 Akt, mTOR, and the estrogen receptor as a signature to predict tamoxifen treatment benefit.
598 Breast Cancer Res Treat **2013**;137:397-406

599 28. Chen H, Mingming C, Pengcheng G, Xiangzhong Z, Ganggang L, Liting W*, et al.* GDC-0941
600 activates integrin linked kinase (ILK) expression to cause resistance to GDC-0941 in breast
601 cancer by the tumor necrosis factor (TNF)-α signaling pathway. Bioengineered **2022**;13:10944-
602 55

603 29. Elder AM, Fairchild HR, Kines KT, Cozzens LM, Becks AR, Slansky JE*, et al.* Semaphorin7A
604 and PD-L1 cooperatively drive immunosuppression during mammary involution and breast
605 cancer. Cell Rep **2025**;44:115676

606 30. Czopik AK, Bynoe MS, Palm N, Raine CS, Medzhitov R. Semaphorin 7A Is a Negative
607 Regulator of T Cell Responses. Immunity **2006**;24:591-600

608 31. Gómez Tejeda Zañudo J, Mao P, Alcon C, Kowalski K, Johnson GN, Xu G*, et al.* Cell Line-
609 Specific Network Models of ER(+) Breast Cancer Identify Potential PI3Kα Inhibitor Resistance
610 Mechanisms and Drug Combinations. Cancer Res **2021**;81:4603-17

611 32. Kines KaF, Heather and Elder, Alan and Cozzens, Lauren and Strugar, Zachary and Porter,
612 Weston and Borges, Virginia and Lyons, Traci, . Aging-Induced Semaphorin 7a Promotes
613 Tgfβ1-Mediated Cell Plasticity and Breast Tumor Metastases. Cell Press Sneak Peak **2024**

614 33. Elder AM, Fairchild HR, Kines KT, Cozzens LM, Becks AR, Lyons TR. Semaphorin7A and
615 PD-L1 cooperatively drive immunosuppression during mammary involution and breast cancer.
616 bioRxiv **2025**:2025.01.03.631229

617 34. Schneider CA, Rasband WS, Eliceiri KW. NIH Image to ImageJ: 25 years of image analysis. Nat
618 Methods **2012**;9:671-5

619 35. DeRose YS, Gligorich KM, Wang G, Georgelas A, Bowman P, Courdy SJ*, et al.* Patient-derived
620 models of human breast cancer: protocols for in vitro and in vivo applications in tumor biology
621 and translational medicine. Curr Protoc Pharmacol **2013**;Chapter 14:Unit14 23

622 36. Massarweh S, Osborne CK, Creighton CJ, Qin L, Tsimelzon A, Huang S*, et al.* Tamoxifen
623 resistance in breast tumors is driven by growth factor receptor signaling with repression of
624 classic estrogen receptor genomic function. Cancer Res **2008**;68:826-33

625 37. Gyorffy B. Survival analysis across the entire transcriptome identifies biomarkers with the
626 highest prognostic power in breast cancer. Comput Struct Biotechnol J **2021**;19:4101-9

627 38. Goldman MJ, Craft B, Hastie M, Repecka K, McDade F, Kamath A*, et al.* Visualizing and
628 interpreting cancer genomics data via the Xena platform. Nat Biotechnol **2020**;38:675-8

629 39. Coarfa C, Grimm SL, Rajapakshe K, Perera D, Lu HY, Wang X*, et al.* Reverse-Phase Protein
630 Array: Technology, Application, Data Processing, and Integration. J Biomol Tech **2021**

631 40. Zheng S, Wang W, Aldahdooh J, Malyutina A, Shadbahr T, Tanoli Z*, et al.* SynergyFinder Plus:
632 Toward Better Interpretation and Annotation of Drug Combination Screening Datasets.
633 Genomics Proteomics Bioinformatics **2022**;20:587-96

634 41. Davis JB, Andes S, Espina V. Reverse Phase Protein Arrays. Methods Mol Biol **2021**;2237:103-
635 22

636 42. Xu W, Yang Z, Lu N. A new role for the PI3K/Akt signaling pathway in the epithelial-
637 mesenchymal transition. Cell Adh Migr **2015**;9:317-24

638 43. Ludwig BS, Kessler H, Kossatz S, Reuning U. RGD-Binding Integrins Revisited: How Recently
639 Discovered Functions and Novel Synthetic Ligands (Re-)Shape an Ever-Evolving Field. Cancers
640 (Basel) **2021**;13

641 44. Jallow F, O'Leary KA, Rugowski DE, Guerrero JF, Ponik SM, Schuler LA. Dynamic
642 interactions between the extracellular matrix and estrogen activity in progression of ER+ breast
643 cancer. Oncogene **2019**;38:6913-25

644 45. Mori H, Chen JQ, Cardiff RD, Pénzváltó Z, Hubbard NE, Schuetter L*, et al.* Pathobiology of the
645 129:Stat1 (-/-) mouse model of human age-related ER-positive breast cancer with an immune
646 infiltrate-excluded phenotype. Breast Cancer Res **2017**;19:102

647 46. Mayer IA, Arteaga CL. The PI3K/AKT Pathway as a Target for Cancer Treatment. Annu Rev
648 Med **2016**;67:11-28

649 47. Technology GC. 2024 Global Cancer Technology. <https://globalcancertechnology.com/>.

650 48. Mori H, Chen JQ, Cardiff RD, Pénzváltó Z, Hubbard NE, Schuetter L*, et al.* Pathobiology of the
651 129:Stat1−/− mouse model of human age-related ER-positive breast cancer with an immune
652 infiltrate-excluded phenotype. Breast Cancer Research **2017**;19:102

653 49. Nieberler M, Reuning U, Reichart F, Notni J, Wester HJ, Schwaiger M*, et al.* Exploring the Role
654 of RGD-Recognizing Integrins in Cancer. Cancers (Basel) **2017**;9

655 50. Pontiggia O, Sampayo R, Raffo D, Motter A, Xu R, Bissell MJ*, et al.* The tumor
656 microenvironment modulates tamoxifen resistance in breast cancer: a role for soluble stromal
657 factors and fibronectin through β1 integrin. Breast Cancer Res Treat **2012**;133:459-71

658 51. Chang DY, Ma WL, Lu YS. Role of Alpelisib in the Treatment of PIK3CA-Mutated Breast
659 Cancer: Patient Selection and Clinical Perspectives. Ther Clin Risk Manag **2021**;17:193-207

660 52. Armaghani AJ, Han HS. Alpelisib in the Treatment of Breast Cancer: A Short Review on the
661 Emerging Clinical Data. Breast Cancer (Dove Med Press) **2020**;12:251-8

662 53. Wilhoit T, Patrick JM, May MB. Alpelisib: A Novel Therapy for Patients With PIK3CA-
663 Mutated Metastatic Breast Cancer. J Adv Pract Oncol **2020**;11:768-75

664

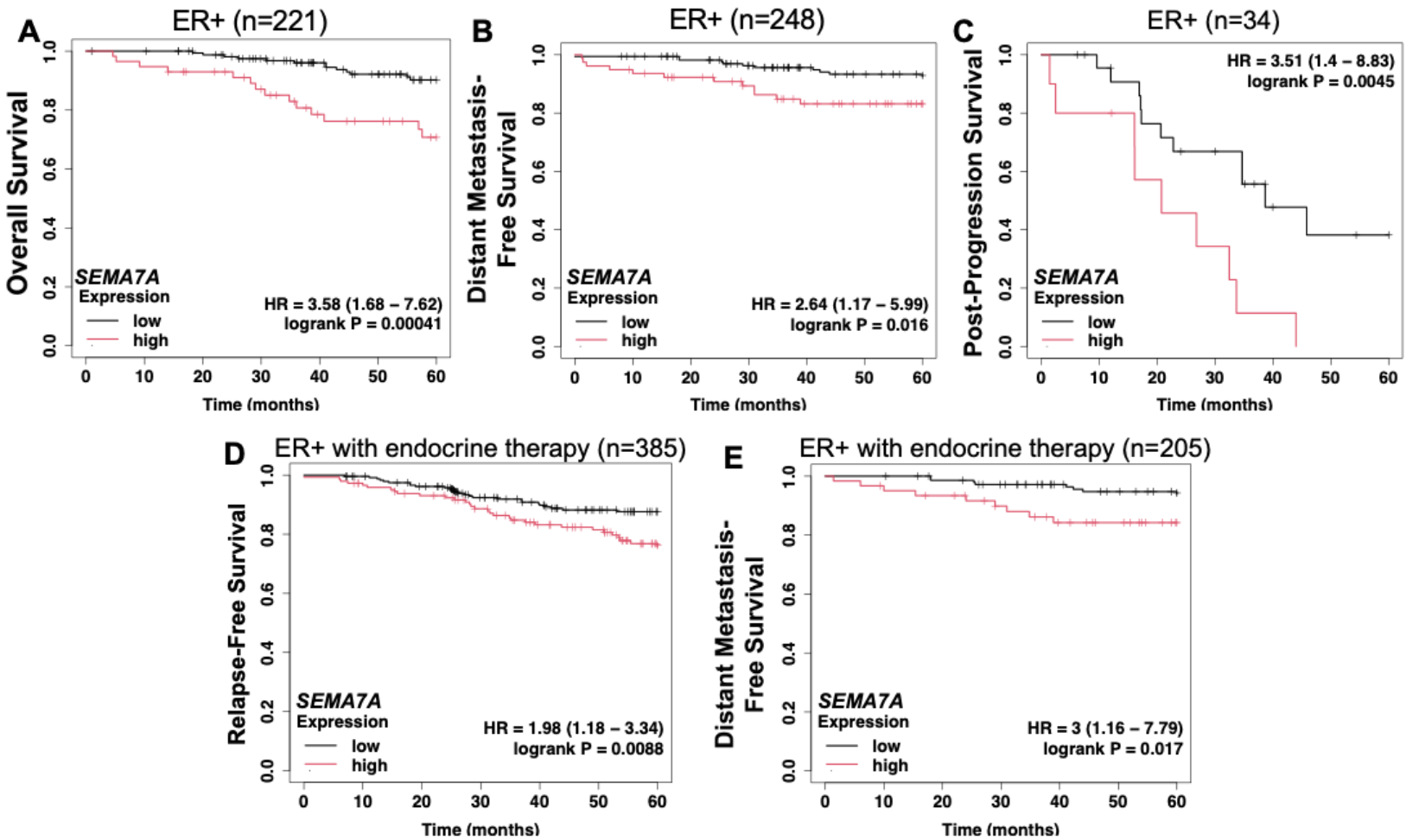

Figure 1. SEMA7A is expressed in ER+ breast cancer and is associated with decreased 5-year patient survival.

Survival analysis was done via Kaplan-Meier Plotter, which was assessed for *SEMA7A* mRNA expression levels in breast cancer patients in the ER+ subtype dataset (n=3499). Data are shown as KM plots; curves are stratified by *SEMA7A* high (red) and low (black) expression. Hazard ratios (HR) and log-rank p-values are included.

A) Overall survival; ER+ subtype (OS; n=221).

B) Distant metastasis-free survival; ER+ subtype (DMFS; n=248).

C) Post-progression survival; ER+ subtype (PPS; n=34).

Further analysis was done within the ER+ subtype to include only patients who had received endocrine therapy (n=1831).

D) Relapse-free survival; ER+ and received endocrine therapy (RFS; n=385).

E) Distant metastasis-free survival: ER+ and received endocrine therapy (DMFS; n=205).

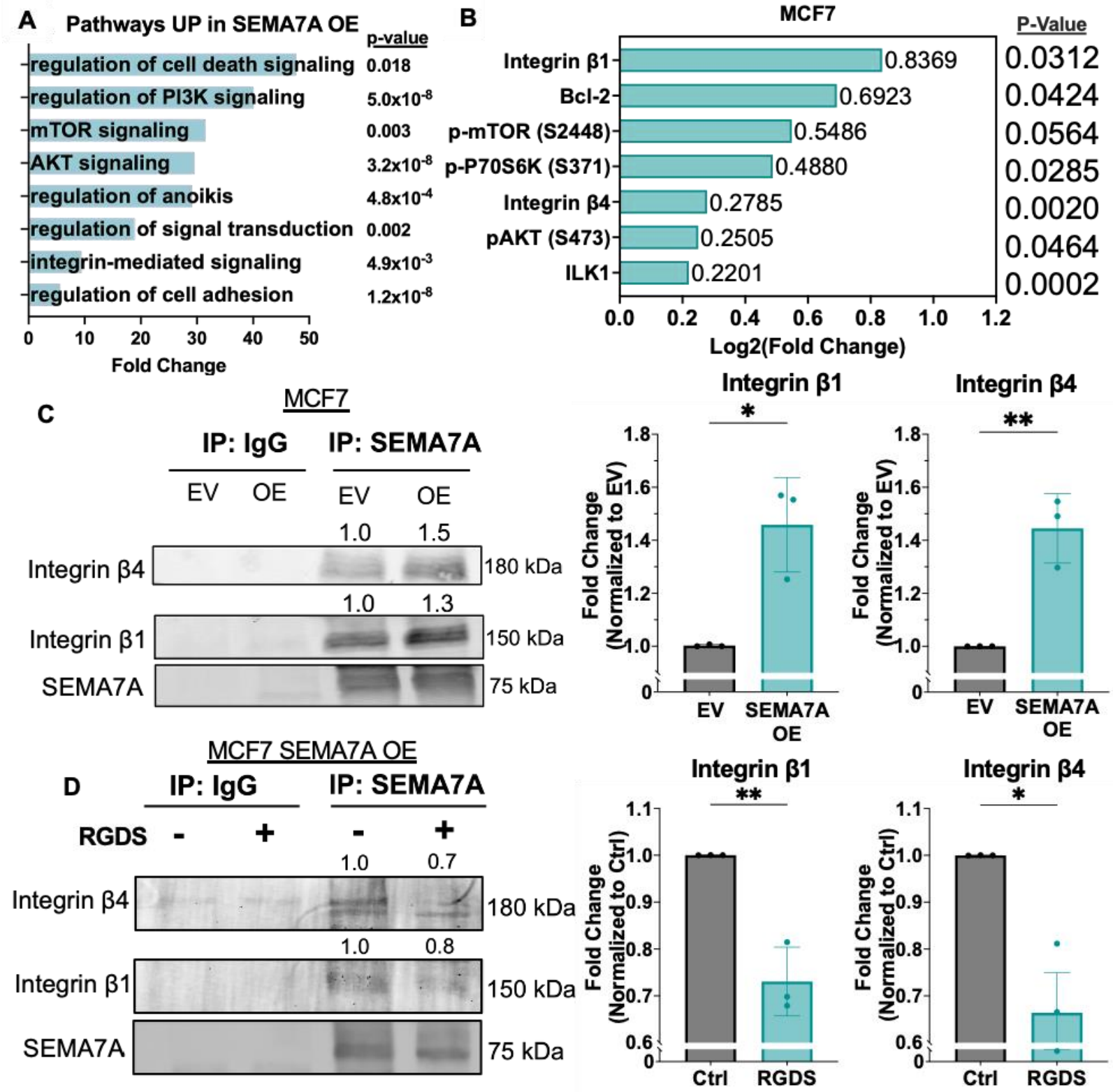

Figure 2. SEMA7A activates AKT signaling and binds to Integrins β1 and β4 via RGD in ER+ tumor cells.

A) Gene Ontology (GO) Pathway Analysis of RPPA results, showing top pathways upregulated in MCF7 SEMA7A OE cell lysates, as fold change compared to EV, $p<0.05$.

B) Log2(fold change) of integrin and AKT-related proteins in MCF7 SEMA7A OE versus EV lysates from RPPA-1 data. Multiple two-tailed unpaired t-tests.

C) Immunoblot for Integrin β4, Integrin β1 and SEMA7A in elutions following CoIP of MCF7 EV and SEMA7A OE lysates for IgG or SEMA7A. ii. Quantification of IP shown as fold change compared to EV. Two-tailed unpaired t-test.

D) Immunoblot for Integrin β4, Integrin β1 and SEMA7A in elutions following CoIP of MCF7 lysates for IgG or SEMA7A, after treatment with PBS (-) or 50 μM RGDS (+). Quantification of IP shown as fold change compared to control. Two-tailed unpaired t-test.

Error bars are mean +/- SD. *$p<0.05$, **$p<0.01$, ***$p<0.001$, ****$p<0.0001$.

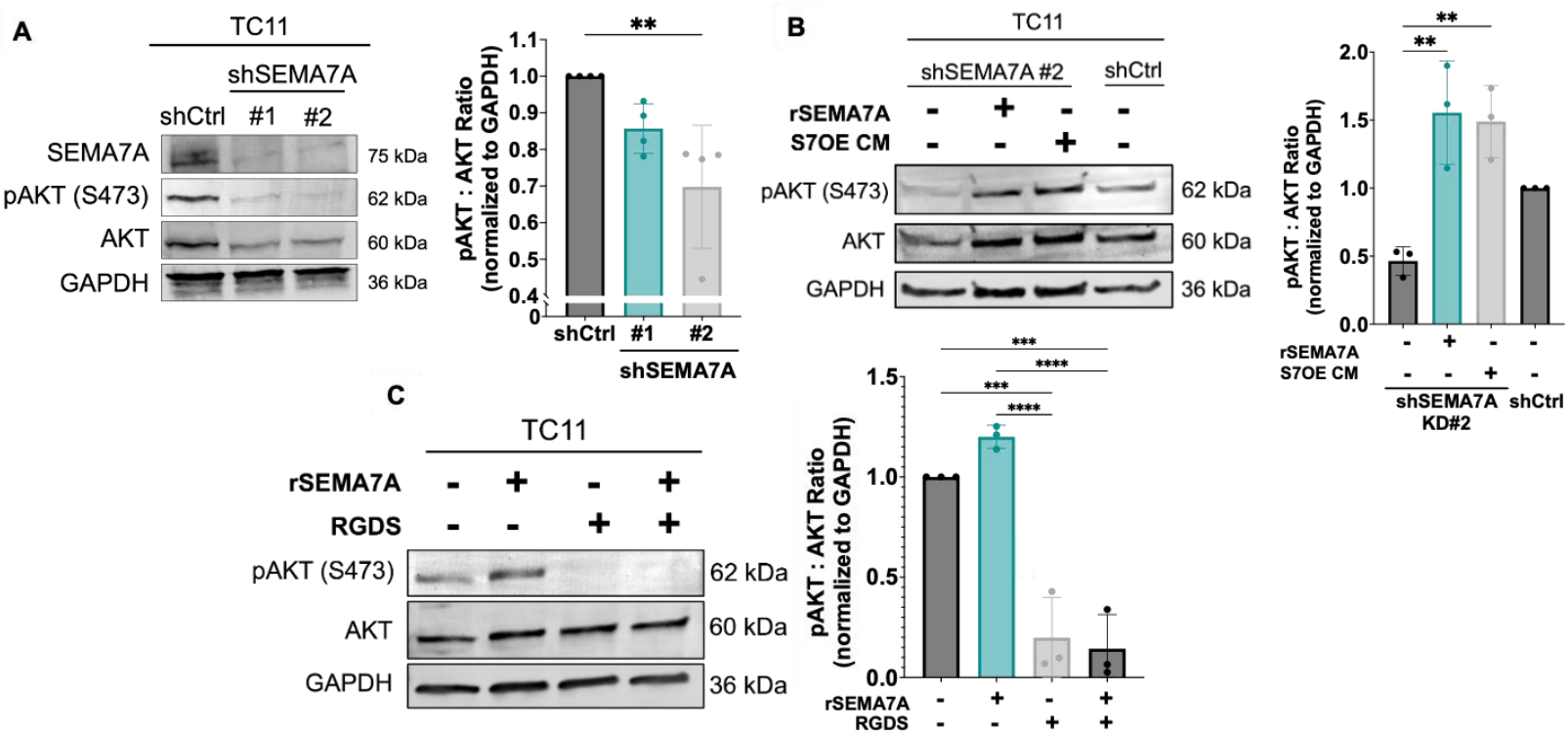

Figure 3. SEMA7A-mediated activation of AKT is dependent on RGD binding in ER+ tumor cells.

A) Representative immunoblot for pAKT (S473), AKT and GAPDH in TC11 shCtrl and shSEMA7A (KD#1 and KD#2) cell lines. Bar graph: ratio of pAKT to total AKT. Ordinary one-way ANOVA with Tukey's multiple comparisons test.

B) Representative immunoblot for pAKT (S473), AKT and GAPDH in TC11 shCtrl and shSEMA7A KD#2 cell lines after treatment for 24 hours with 20 µg/mL purified rSEMA7A, or conditioned media from SEMA7A OE cells (S7OE CM). Bar graph: ratio of pAKT to total AKT. Ordinary one-way ANOVA with Tukey's multiple comparisons test.

C) Representative immunoblot for pAKT (S473), AKT and GAPDH in TC11 WT cell lysates after treatment for 1 hour with 20 µg/mL rSEMA7A, 50 µM RGDS peptide, or both. Bar graph: ratio of pAKT to total AKT. Ordinary one-way ANOVA with Tukey's multiple comparisons test.

Error bars are mean +/- SD. *p<0.05, **p<0.01, ***p<0.001, ****p<0.0001.

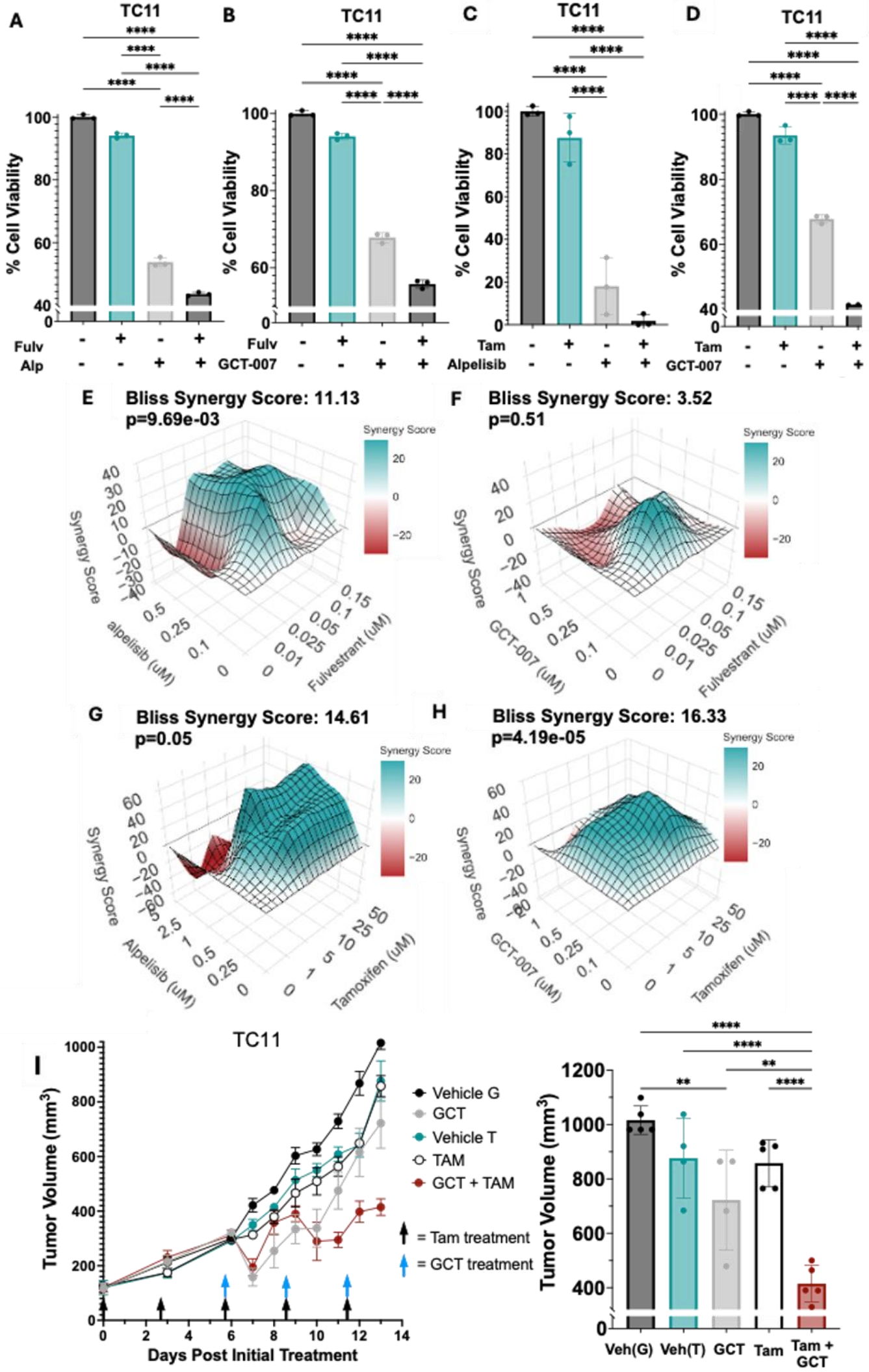
A
TC11
% Cell Viability
Fulv
Alp
B
TC11
% Cell Viability
Fulv
GCT-007
C
TC11
% Cell Viability
Tam
Alpelisib
D
TC11
% Cell Viability
Tam
GCT-007
E
Bliss Synergy Score: 11.13
p=9.69e-03
Synergy Score
alpelisib (uM)
Fulvestrant (uM)
F
Bliss Synergy Score: 3.52
p=0.51
Synergy Score
GCT-007 (uM)
Fulvestrant (uM)
G
Bliss Synergy Score: 14.61
p=0.05
Synergy Score
Alpelisib (uM)
Tamoxifen (uM)
H
Bliss Synergy Score: 16.33
p=4.19e-05
Synergy Score
GCT-007 (uM)
Tamoxifen (uM)
I
TC11
Tumor Volume (mm³)
Days Post Initial Treatment
Vehicle G
GCT
Vehicle T
TAM
GCT + TAM
= Tam treatment
= GCT treatment
Tumor Volume (mm³)
Veh(G)
Veh(T)
GCT
Tam
Tam + GCT

Figure 4. SEMA7A+ tumor growth is inhibited by combination treatment with endocrine therapy and PI3K inhibitors.

A) Percent cell viability quantified via crystal violet staining after 48-hour treatment of TC11 cells with DMSO, 8nM fulvestrant, 1μM alpelisib, or the combination, normalized to control. Ordinary one-way ANOVA with Tukey's multiple comparisons test.

B) Percent cell viability quantified via crystal violet staining after 48-hour treatment of TC11 cells with DMSO, 8nM fulvestrant, 0.3μM GCT-007, or the combination, normalized to control. Ordinary one-way ANOVA with Tukey's multiple comparisons test.

C) Percent cell viability quantified via crystal violet staining after 48-hour treatment of TC11 cells with DMSO, 5 μM 4-hydroxytamoxifen, 1μM alpelisib, or the combination, normalized to control. Ordinary one-way ANOVA with Tukey's multiple comparisons test.

D) Percent cell viability quantified via crystal violet staining after 48-hour treatment of TC11 cells with DMSO, 5 μM 4-hydroxytamoxifen, 0.3 μM GCT-007, or the combination, normalized to control. Ordinary one-way ANOVA with Tukey's multiple comparisons test.

E) Bliss synergy score for fulvestrant and alpelisib in TC11 cells.

F) Bliss synergy score for fulvestrant and GCT-007 in TC11 cells.

G) Bliss synergy score for (4-hydroxy)tamoxifen and alpelisib in TC11 cells.

H) Bliss synergy score for (4-hydroxy)tamoxifen and GCT-007 in TC11 cells.

I) Average TC11 tumor volume over time in FVB/N mice, in groups treated with Vehicle, GCT-007, tamoxifen, or the combination. GCT = GCT-007, TAM = tamoxifen. Bar graph: tumor volume at the study endpoint (Day 13). Ordinary one-way ANOVA with Tukey's multiple comparisons test.

Error bars are mean +/- SD (A-D), or mean +/- SEM (I). *$p<0.05$, **$p<0.01$, ***$p<0.001$, ****$p<0.0001$.

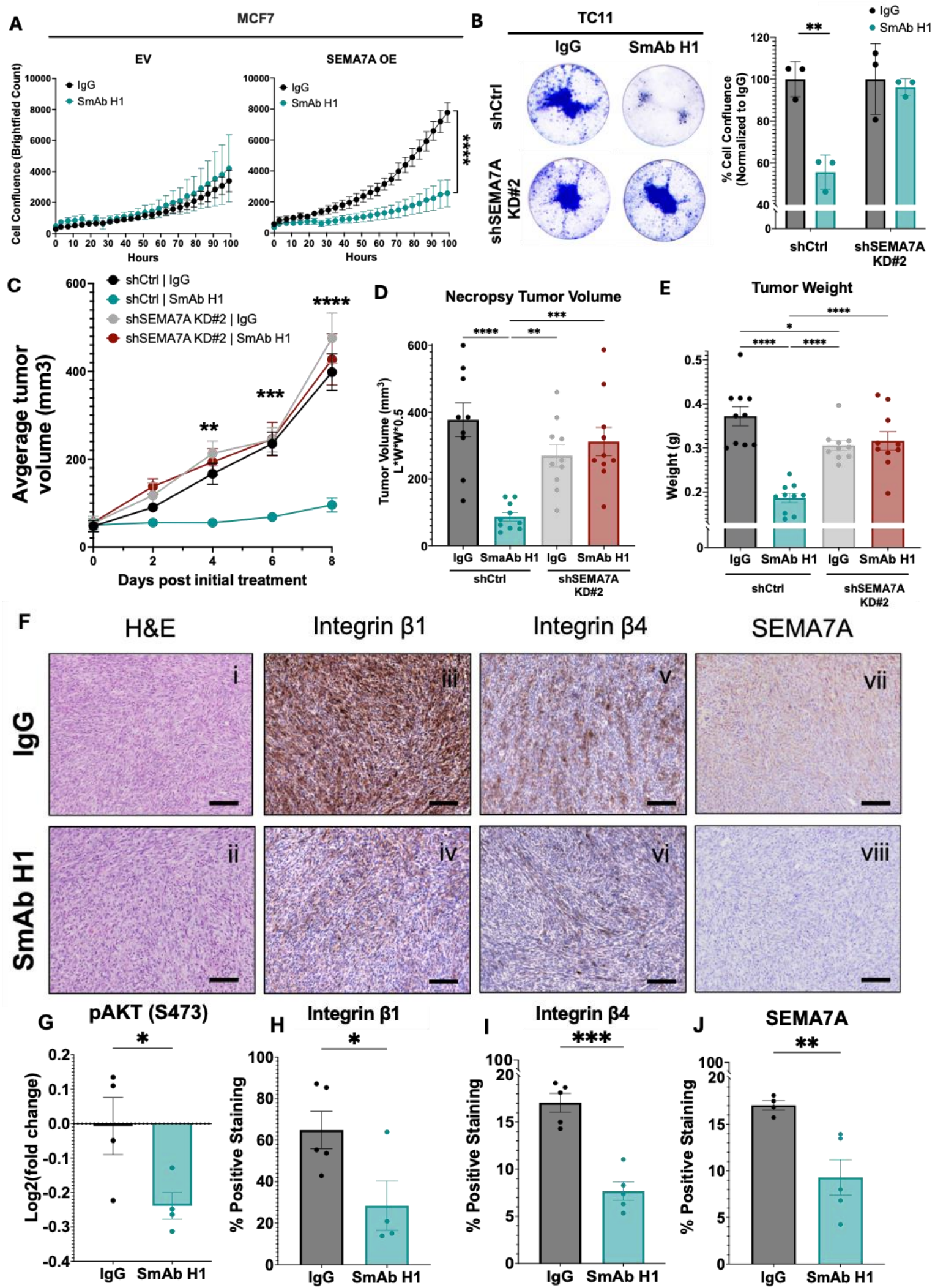
A
MCF7
EV
SEMA7A OE
IgG
SmAb H1
Cell Confluence (Brightfield Count)
Hours
****
B
TC11
IgG
SmAb H1
shCtrl
shSEMA7A KD#2
% Cell Confluence (Normalized to IgG)
**
C
shCtrl | IgG
shCtrl | SmAb H1
shSEMA7A KD#2 | IgG
shSEMA7A KD#2 | SmAb H1
Avgerage tumor volume (mm3)
Days post initial treatment
D
Necropsy Tumor Volume
Tumor Volume (mm³) L*W*W*0.5
E
Tumor Weight
Weight (g)
F
H&E
Integrin β1
Integrin β4
SEMA7A
IgG
SmAb H1
i
ii
iii
iv
v
vi
vii
viii
G
pAKT (S473)
Log2(fold change)
H
Integrin β1
% Positive Staining
I
Integrin β4
J
SEMA7A

Figure 5. Direct inhibition of SEMA7A using a monoclonal antibody (SmAb H1) reduces tumor growth and AKT signaling in ER+ BC.

A) Brightfield cell count measured by BioSpa Live Imaging over 96 hours of MCF7 EV and SEMA7A OE cells treated with mouse IgG1 or 1 μM SmAb H1. Two-tailed unpaired t-test at time = 96 hours.

B) Representative crystal violet staining of TC11 shCtrl and shSEMA7A KD#2 cells after treatment for 48 hours with mouse IgG1 or 1 μM SmAb H1. Bar graph: quantification of all replicates. Ordinary one-way ANOVA with Tukey's multiple comparisons test.

C) Average tumor volume in TC11 tumor-bearing mice over time, with groups receiving IgG1 or SmAb H1 (n=5 per group). Two-tailed unpaired t-test at day 4, 6, and 8 between (shCtrl) IgG and (shCtrl) SmAb H1 groups..

D) Tumor volume calculated using necropsy tumor photos in TC11 shCtrl and shSEMA7A-tumor bearing mice over time with groups receiving IgG1 or SmAb H1 (n=10 per group). Ordinary one-way ANOVA with Tukey's multiple comparisons test.

E) Weight of the tumor (and attached mammary gland) at study endpoint (n=10/group). Ordinary one-way ANOVA with Tukey's multiple comparisons test.

F) Immunohistochemistry staining of ex vivo TC11 tumors from IgG-treated and SmAb H1-treated groups. Scale bars = 50μm. Hematoxylin and eosin (H&E) staining (i-ii), active integrin B1 (9EG7) staining; brown (iii-iv), integrin B4 staining; brown (v-vi), and SEMA7A staining; brown (vii-viii).

G) Log2(fold change) of pAKT (S473) expression in SmAb H1-treated versus IgG-treated TC11 tumors from RPPA-2 data. Two-tailed unpaired t-test.

H) Quantification of 9EG7 (active ITGB1) IHC staining from all tumors (n=5 per group); Percent positive out of tumor area. Two-tailed unpaired t-test.

I) Quantification of ITGB4 IHC staining from all tumors (n=5 per group); Percent positive out of tumor area. Two-tailed unpaired t-test.

J) Quantification of SEMA7A IHC staining from all tumors (n=5 per group); percent positive out of tumor area. Two-tailed unpaired t-test.

Error bars are mean +/- SD (A-B), or mean +/- SEM (C-E, G-I). *$p<0.05$, **$p<0.01$, ***$p<0.001$, ****$p<0.0001$.

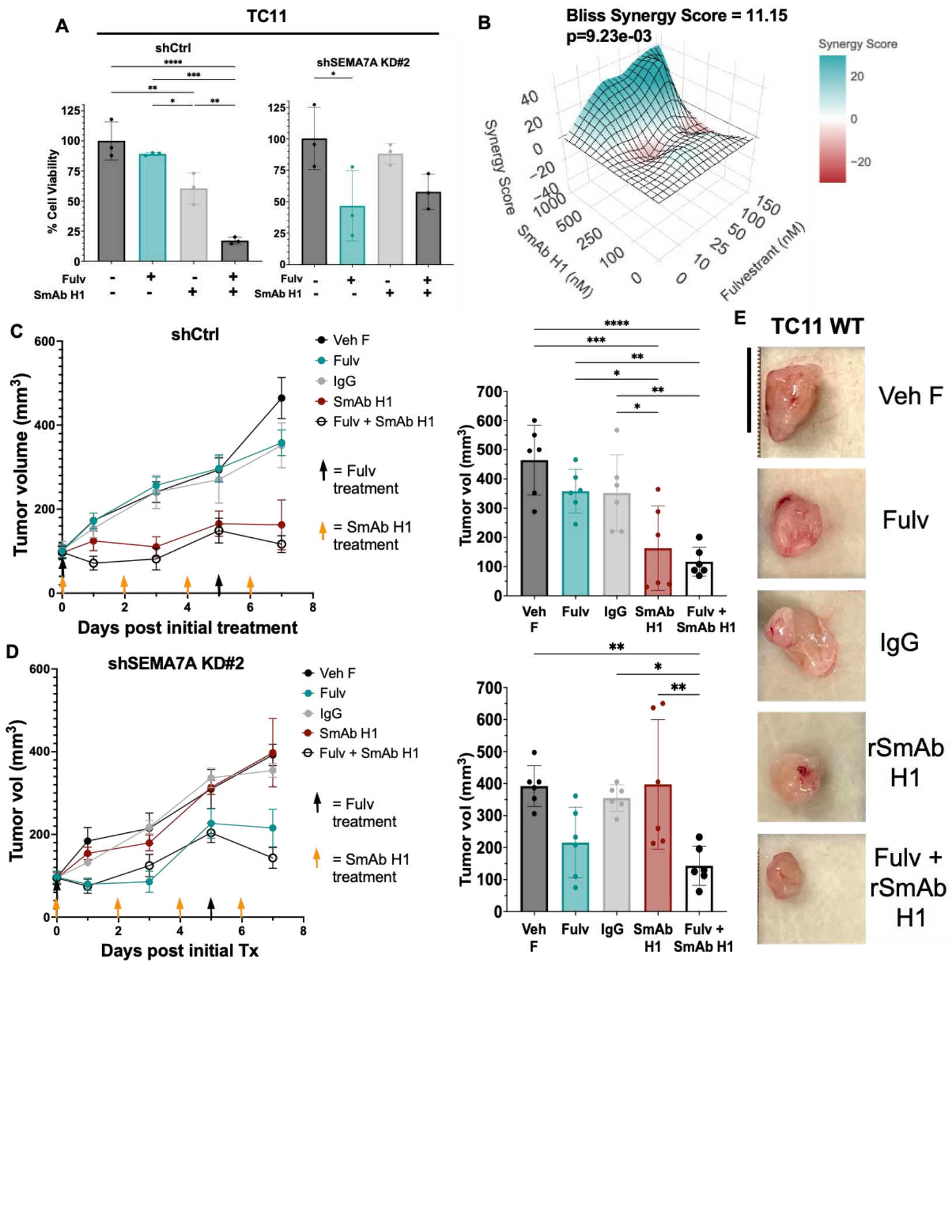
A
TC11
shCtrl
shSEMA7A KD#2
% Cell Viability
Fulv
SmAb H1
B
Bliss Synergy Score = 11.15
p=9.23e-03
Synergy Score
SmAb H1 (nM)
Fulvestrant (nM)
C
shCtrl
Tumor volume (mm³)
Days post initial treatment
Veh F
Fulv
IgG
SmAb H1
Fulv + SmAb H1
= Fulv treatment
= SmAb H1 treatment
Tumor vol (mm³)
Veh F
Fulv
IgG
SmAb H1
Fulv + SmAb H1
D
shSEMA7A KD#2
Tumor vol (mm³)
Days post initial Tx
E
TC11 WT
Veh F
Fulv
IgG
rSmAb H1
Fulv + rSmAb H1

Figure 6. Combination treatment with fulvestrant and SmAb H1 reduces SEMA7A+ ER+ tumor growth.

A) Cell viability quantified via crystal violet staining after 48-hour treatment of TC11 shCtrl and TC11 shSEMA7A KD#2 cells with DMSO, 8 nM fulvestrant, 1μM SmAb H1, or the combination, normalized to control. Ordinary one-way ANOVA with Tukey's multiple comparisons test.

B) Bliss synergy score for fulvestrant and SmAb H1 in TC11 cells.

C) Average tumor volume in TC11 shCtrl tumor-bearing FVB/N mice over time with groups receiving Vehicle F, IgG1, fulvestrant, SmAb H1 or the combination (n=5 per group). Bar graph: tumor volume at study endpoint (Day 7). Ordinary one-way ANOVA with Tukey's multiple comparisons test.

D) Average tumor volume in TC11 shSEMA7A KD#2 tumor-bearing FVB/N mice over time with groups receiving Vehicle F, IgG1, fulvestrant, SmAb H1 or the combination (n=5 per group). Bar graph: tumor volume at study endpoint (Day 7). Ordinary one-way ANOVA with Tukey's multiple comparisons test.

E) Representative photographs of harvested TC11 tumors treated with Vehicle F, IgG1, fulvestrant, rSmAb H1 or the combination (n=5 per group). Scale bar = 1cm.

Error bars are mean +/- SD (A), or mean +/- SEM (C-D). *$p<0.05$, **$p<0.01$, ***$p<0.001$, ****$p<0.0001$.